Metallomics

Accepted Manuscript

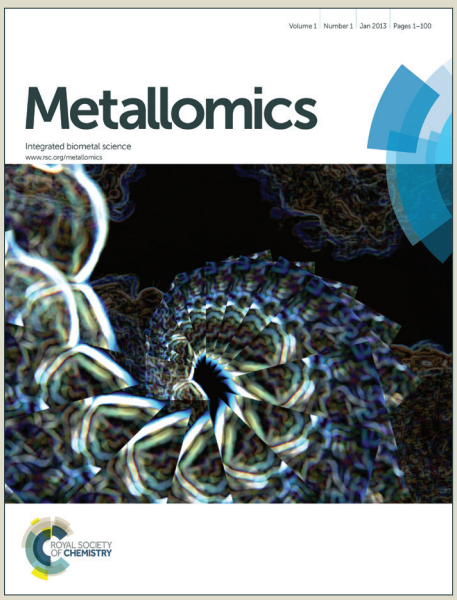

ROYAL SOCIETY OF CHEMISTRY

www.rsc.org/metallomics

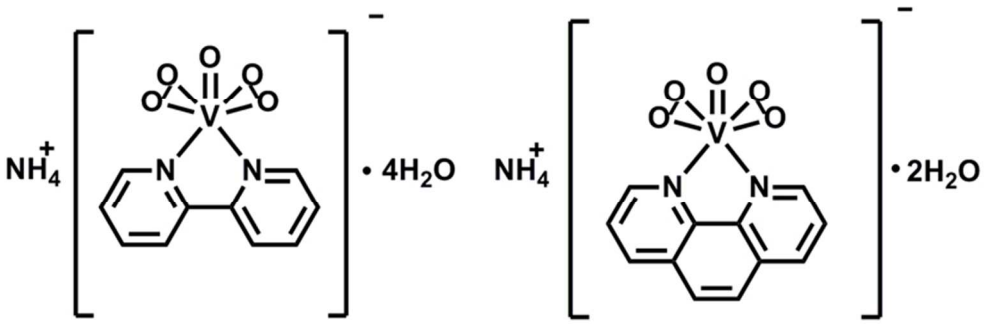

1 2

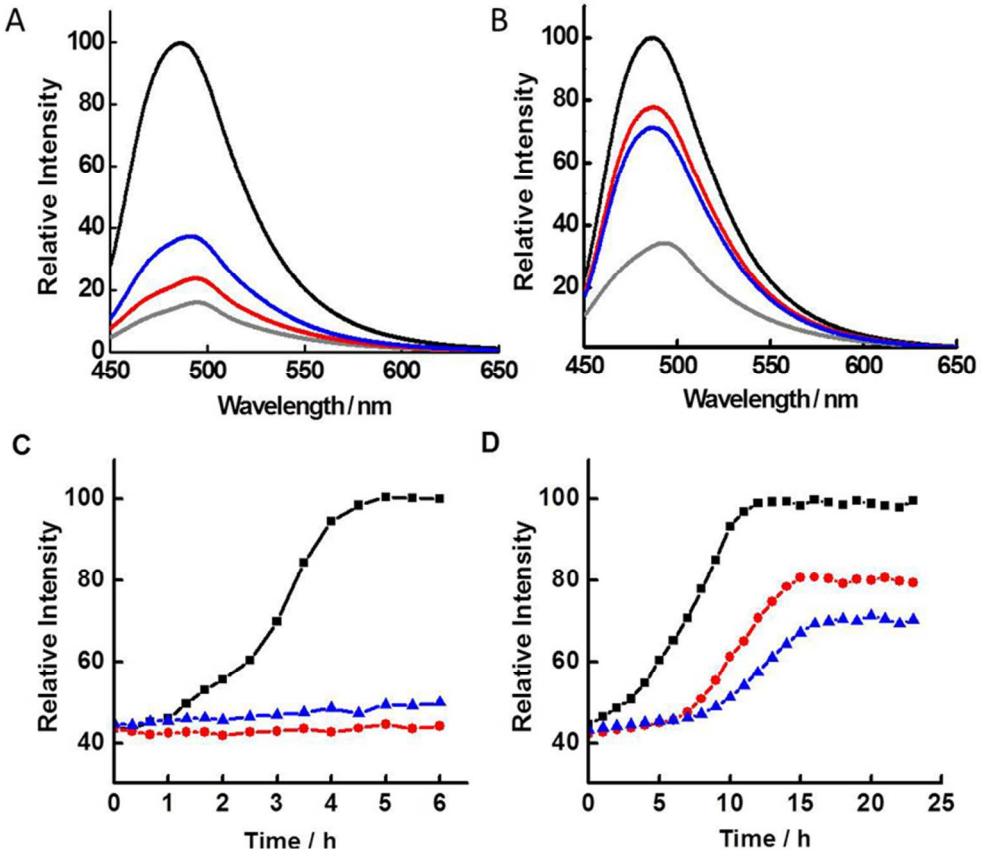

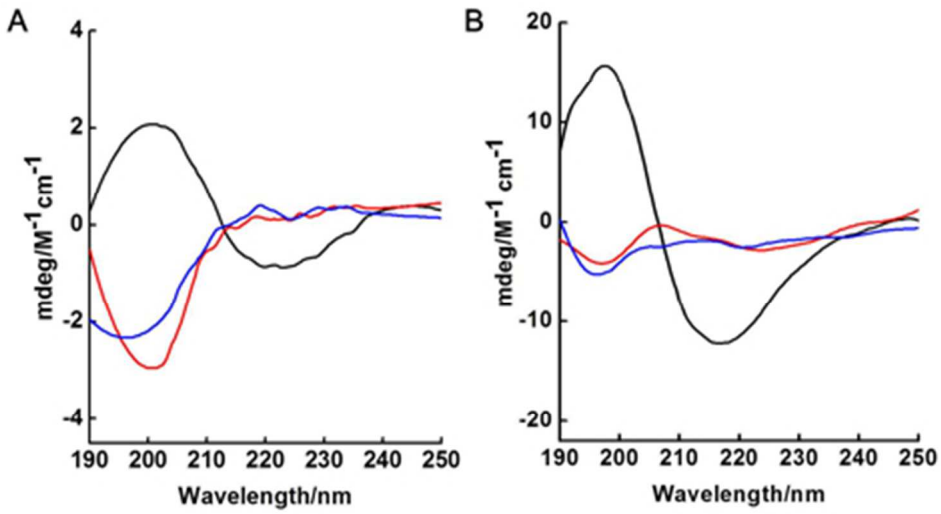

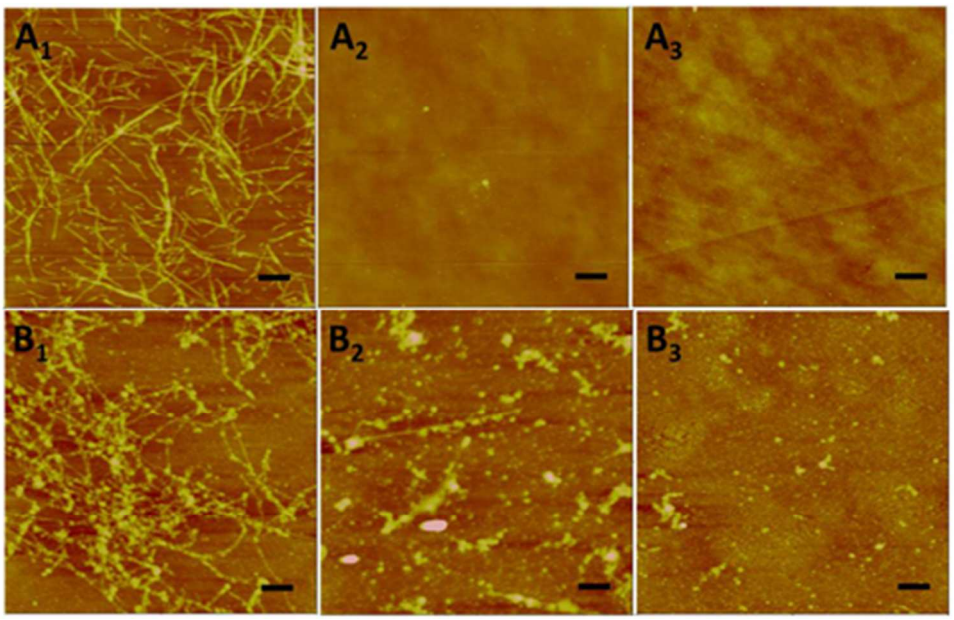

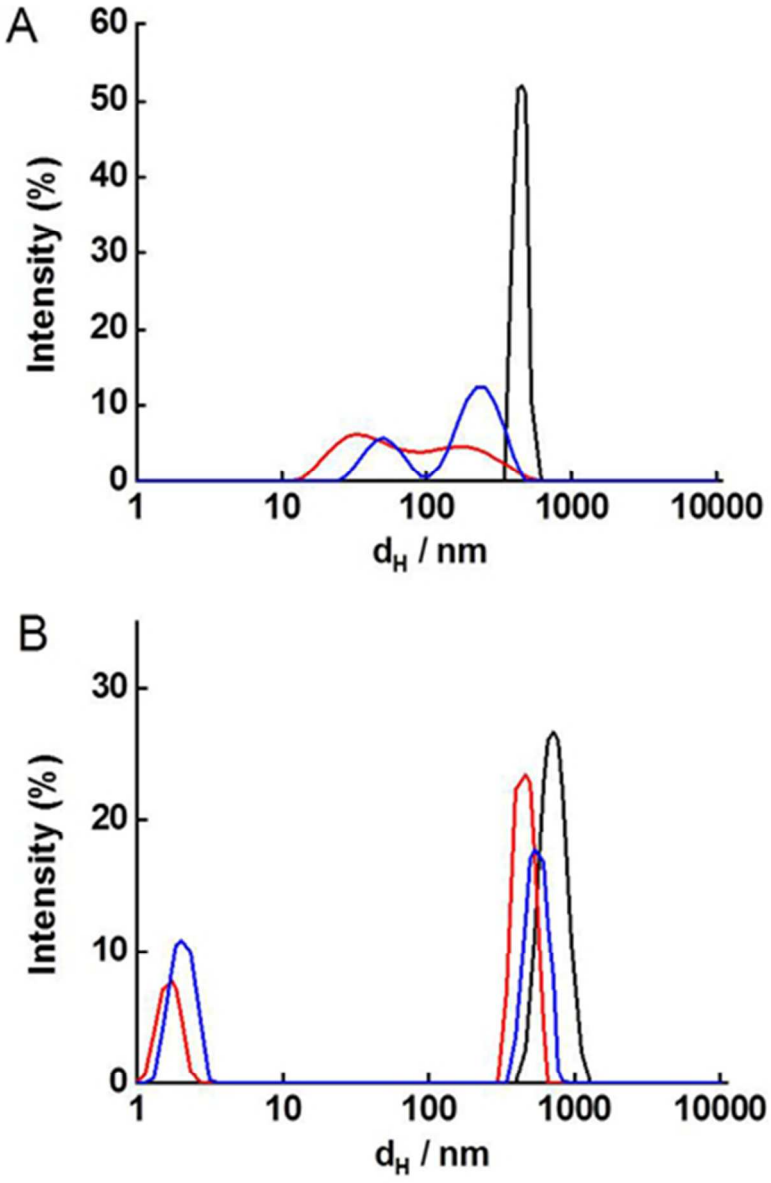

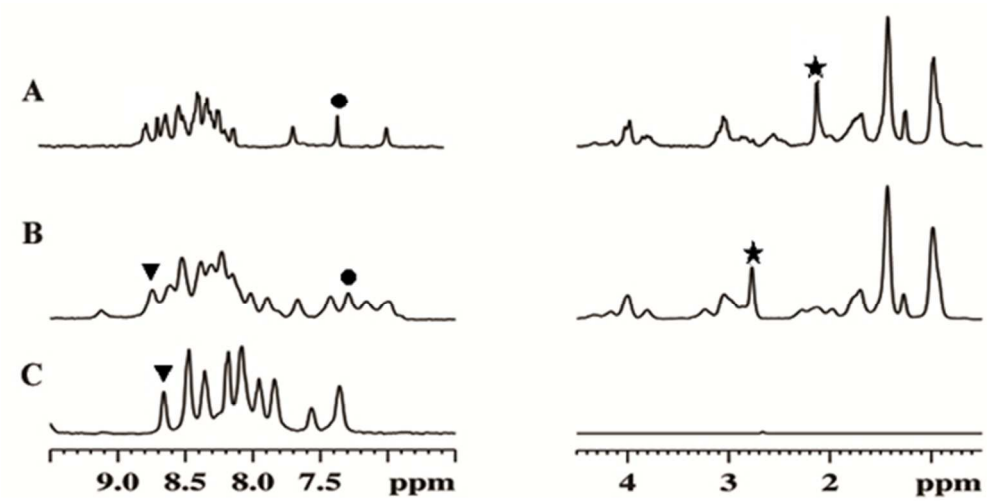

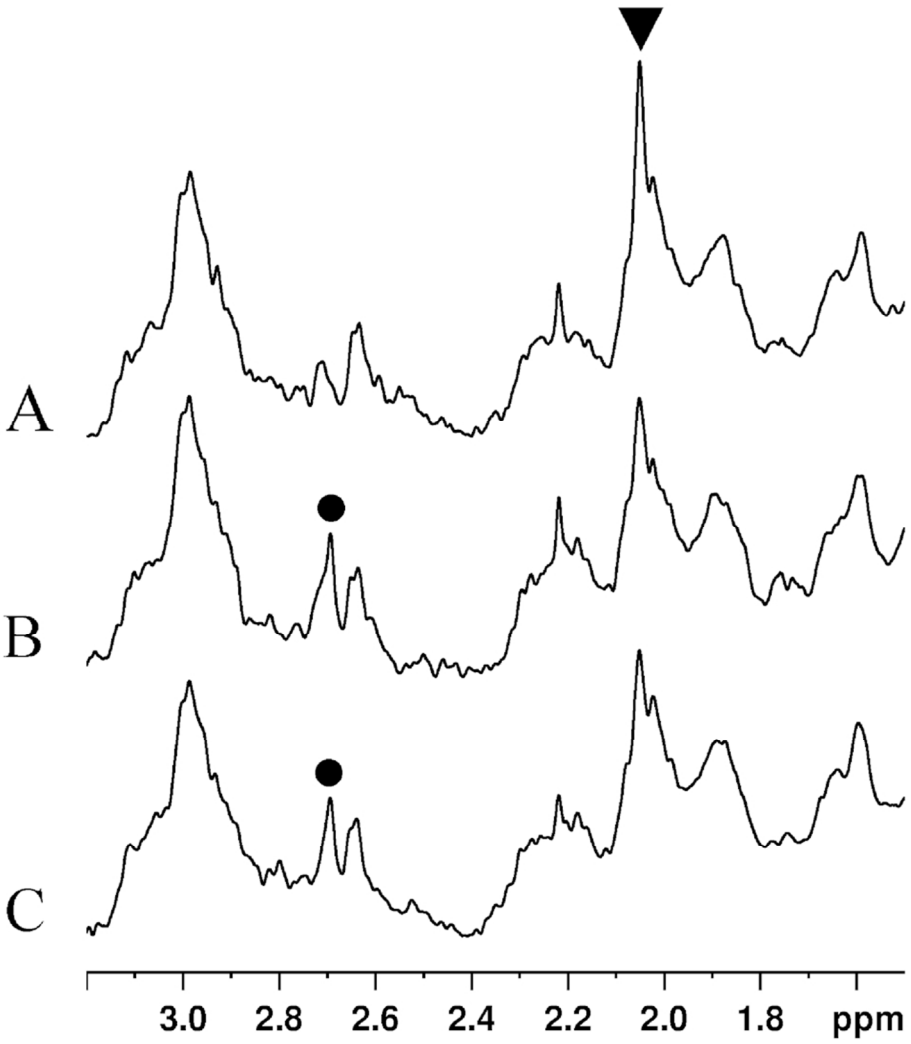

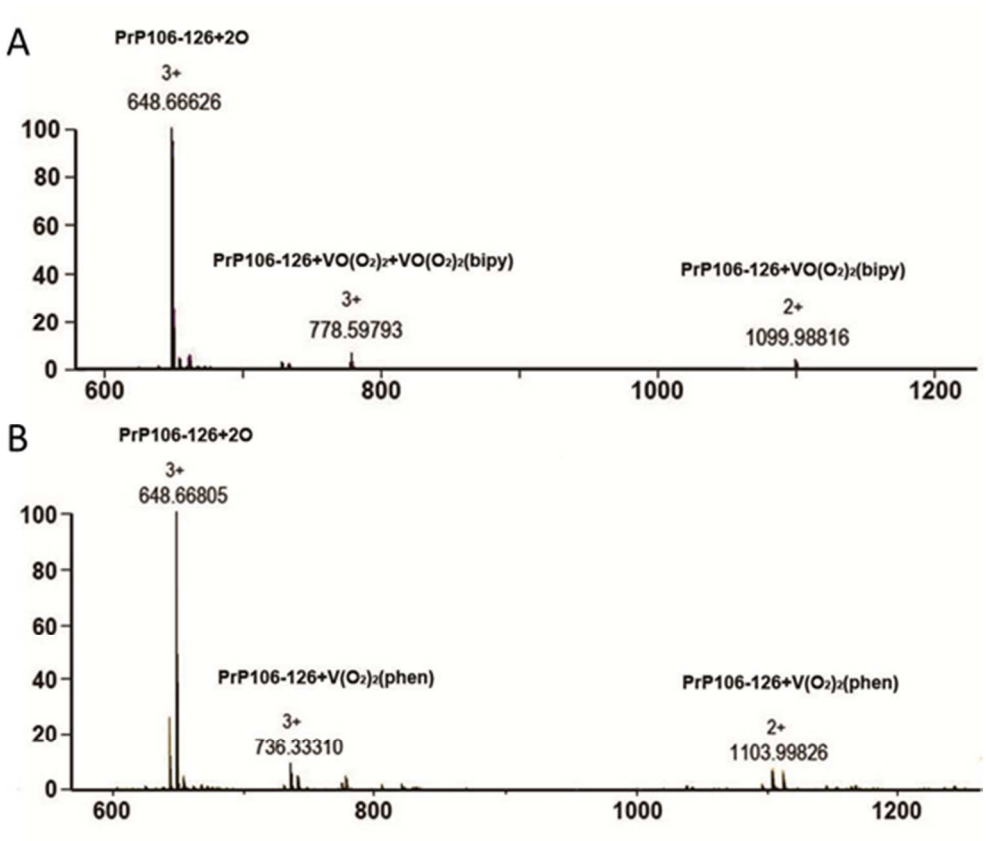

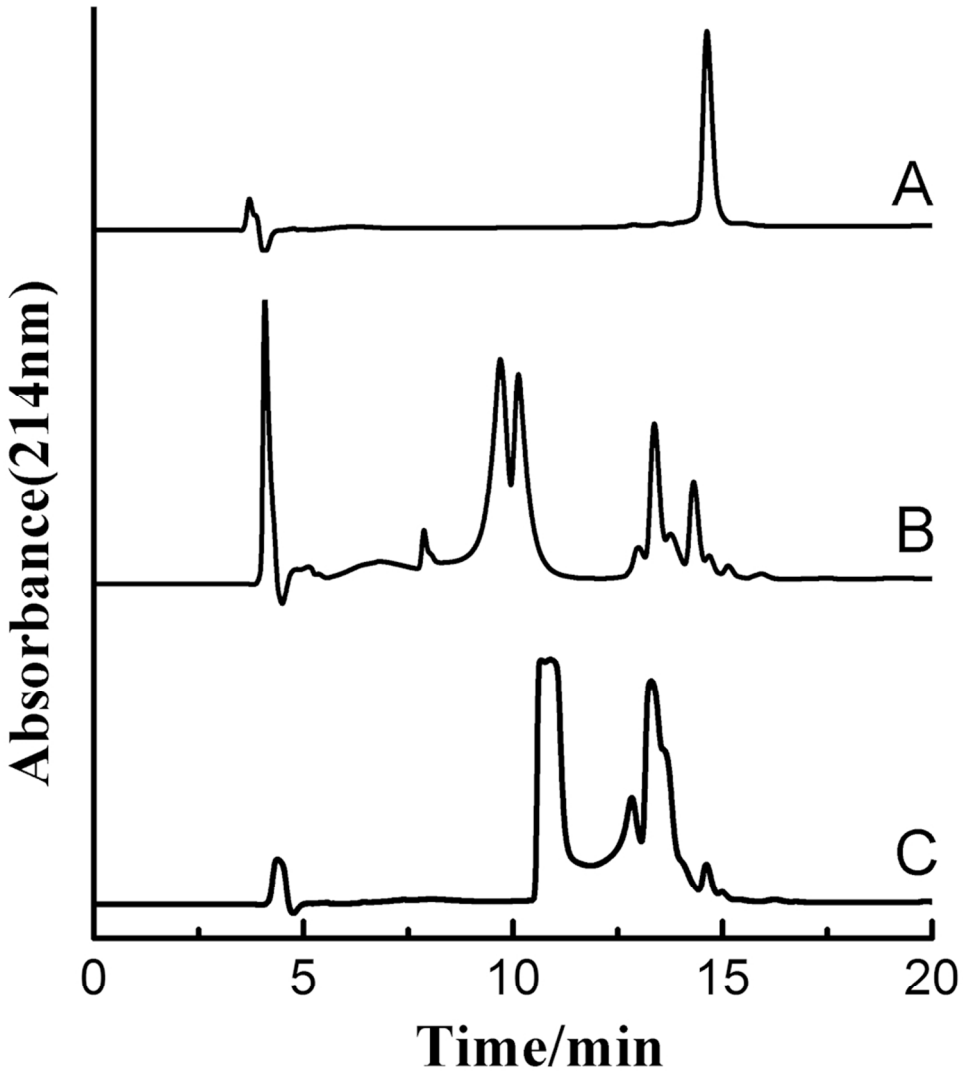

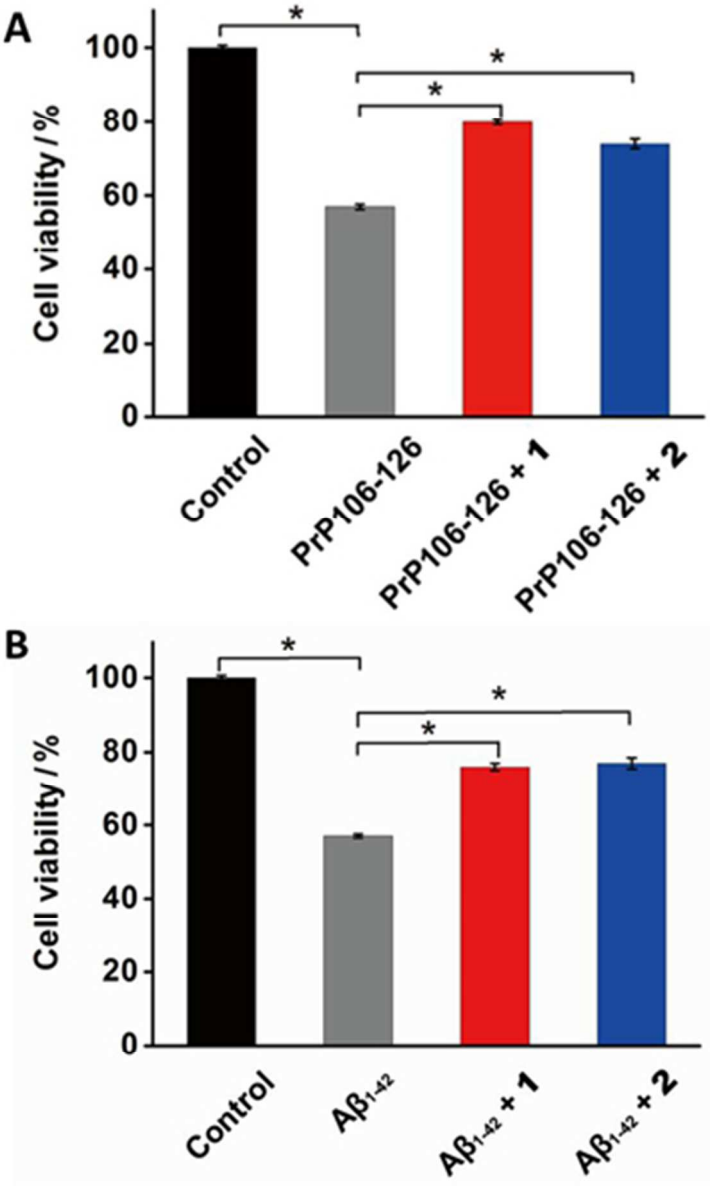

Methionine Oxidation of Amyloid Peptides by Peroxovanadium Complexes: Inhibition of Fibril Formation through a Distinct Mechanism

Lei He[$], Xuesong Wang[$], Dengsen Zhu, Cong Zhao, Weihong Du[*]

Department of Chemistry, Renmin University of China, Beijing, 100872, China

Keywords : Peroxovanadium complexes, methionine oxidation, amyloid peptides, fibril formation, inhibition.

[$] Contributed equally to this paper.

[*]Corresponding Author**.** E-mail for W. Du: whdu@chem.ruc.edu.cn

Abstract

Fibril formation of amyloid peptides is linked to a number of pathological states. The prion protein (PrP) and amyloid-β (Aβ) are two remarkable examples that are correlated with prion disorders and Alzheimer's disease, respectively. Metal complexes, such as those formed by platinum and ruthenium compounds, can act as inhibitors against peptide aggregation primarily through metal coordination. This study revealed the inhibitory effect of two peroxovanadium complexes, $(NH_4)[VO(O_2)_2(bipy)]\cdot 4H_2O$ (**1**) and $(NH_4)[VO(O_2)_2(phen)]\cdot 2H_2O$ (**2**), on amyloid fibril formation of PrP106-126 and $A\beta_{1-42}$ *via* site-specific oxidation of methionine residues, besides direct binding of the complexes with the peptides. Complexes **1** and **2** showed higher anti-amyloidogenic activity on PrP106-126 aggregation than on $A\beta_{1-42}$, though their regulation on the cytotoxicity induced by the two peptides could not be differentiated. The action efficacy may be attributed to the different molecular structures of the vanadium complex and the peptide sequence. Results reflected that methionine oxidation may be a crucial action mode in inhibiting amyloid fibril formation. This study offers a possible application value for peroxovanadium complexes against amyloid proteins.

Introduction

Protein misfolding is associated with a number of pathological states in humans and other animals. For instance, abnormal aggregation of amyloid-β (Aβ) peptide,[1] α-synuclein,[2] and human islet amyloid polypeptide (hIAPP) are correlated to Alzheimer's disease (AD), Parkinson's disease, and type II diabetes, respectively.[3] Although these diseases have different target proteins, their molecular mechanisms of action are similar and involve the accumulation of large deposits; this process is generally referred to as amyloidogenesis.[4]

Prion diseases or transmissible spongiform encephalopathies are protein misfolding-related diseases.[5] They are characterized by conformational change of a host-encoded protein - prion protein (PrP) from the normal form PrP^{C} (cellular) in the non-infected host to the abnormal isoform PrP^{Sc} (scrapie). PrP^{Sc} has physical properties that are profoundly different from the native PrP^{C} form and is considered as an infectious agent.[6] Although PrP^{C} and PrP^{Sc} have identical primary structures, their secondary structure elements are diverse. With significantly more β sheets and less α helix structures, PrP^{Sc} accumulates in the central nervous system of affected individuals, accompanying nerve cell loss.[7] PrP106-126 is an N-terminal segment of the full-length PrP that resembles PrP^{Sc} in many physicochemical and biological properties, such as cellular toxicity, fibrillogenesis, and membrane-binding affinity.[8–14] These observations suggest that PrP106-126 is a crucial fragment to the physicochemical and pathogenic properties of PrP^{Sc}. Although the short peptide cannot represent PrP^{Sc} entirely, PrP106-126 is commonly used as a research model in investigating neurodegeneration in prion diseases because it encompasses a core structure with a typical hydrophobic region that induces protein conformational change.[15–18]

Studies on drugs that can interfere with amyloid formation and eliminate misfolded aggregates are currently being conducted. A variety of inhibitors against amyloidogenic proteins

have been studied in recent years. Small molecules, short peptides, and immunotherapies have been designed to inhibit and/or reverse the conformational changes that result in formation of the pathological protein conformer and its sequential fibril.[19,20] Among potential therapeutic agents, metal complexes, such as those of Pt, Ru, and Cu, show a vital role in inhibiting the aggregation of amyloid proteins.[21–27] The inhibition is primarily caused by the duplex function of metal coordination and ligand hydrophobic effect. However, whether other interaction modes act on the aggregation behavior of amyloids through binding of metal complexes is unclear.

Currently, numerous vanadium compounds, including vanadate, vanadyl sulfate, and several vanadium complexes with organic ligands, demonstrate promising antidiabetic properties.[28–35] Their complexes have been studied as potential therapeutics. A few studies have documented that several forms of vanadium, particularly peroxovanadium species, mimic insulin *via* phosphotyrosine phosphatase inhibition and prevent cancerous tumor growth by inducing DNA cleavage.[36,37] The novel medicinal potential of vanadium compounds has attracted increasing attention in the treatment of endemic diseases in tropical countries, such as Chagas disease, leishmaniasis, amoebiasis, and some viral infections, such as Dengue fever, HIV, and SARS.[38–40] Moreover, our recent work has demonstrated that insulin-mimicking vanadium complexes affect hIAPP aggregation, thereby inhibiting the cytotoxicity induced by the polypeptide.[41] These complexes bind to the peptide mainly by hydrophobic and electrostatic interactions.

We selected two peroxovanadium compounds, **1** and **2** (Scheme 1), and studied their interactions with prion neuropeptide (PrP106-126) to explore the effect of vanadium compounds on amyloidogenic proteins. Their interactions with $A\beta_{1-42}$ were also investigated to compare the various influences of peroxovanadium compounds on different types of amyloid protein

aggregation. Results demonstrated that the peroxovanadium complexes can delay the aggregation and inhibit cytotoxicity induced by PrP106-126 and $A\beta_{1-42}$ *via* direct interaction and site-specific oxidation of methionines. However, the efficacy of the peroxovanadium compounds was different for PrP106-126 and $A\beta_{1-42}$, which implies their distinct peptide properties and aggregation behaviors.

Materials and methods

Materials

Human prion neuropeptide PrP106-126 (106-KTNMKHMAGAAAAGAVVGGLG-126) was chemically synthesized and purified by SBS Co., Ltd. (Beijing, China). $A\beta_{1-42}$ (1-DAEFRHDSGYEVHHQKLVFFAEDVGSNKGAIIGLMVGGVVIA-42) was purchased from GL Biochem Co., Ltd. (Shanghai, China). The final products (>95% purity) were identified by high-performance liquid chromatography (HPLC) and mass spectroscopy (MS). All of the other reagents were analytical grade. Dry $A\beta_{1-42}$ was weighed and dissolved in hexafluoroisopropanol for 1 h to remove any preformed aggregates and then lyophilized. The dry peptide was stored at −20 °C before use. For sample preparation, the peptide was dissolved in 20 mM NaOH, diluted at 1:10 with phosphate buffer (pH 7.5), and sonicated in a water bath containing ice for 15 min. The solution was then centrifuged at 12000×*g* for 30 min, and the supernatant was stored on ice. The initial peptide concentration was determined by spectrophotometry at 214 nm using an extinction coefficient of 75,887 L mol^{-1} cm^{-1} for $A\beta_{1-42}$.

Fluorescence spectroscopy

A 30 μM metal compound was added to a 10 μM peptide solution in a 10 mM phosphate buffer at pH 7.5. After a 24 h incubation of the mixture at 310 K, the sample was combined with 10 μM ThT, and its fluorescence was monitored using an F-4500 fluorescence spectrometer (Hitachi, Japan) with a programmable temperature controller (PolyScience, USA). The ThT fluorescence intensity was quantified by determining the average of fluorescence emissions at 484 nm over 10 s at an excitation of 432 nm. The fluorescence intensity of aggregated peptide was set to 100 and relative intensity was obtained taking the peptide alone as control. Data was reported as the average of three experiments. Moreover, the effect of H_2O_2 on peptide aggregation was performed similarly.

For the IC_{50} determination, the initial concentration of peptide was 10 μM, and vanadium complexes were prepared at concentrations 0, 2, 4, 6, 10, 15, 20, 50, and 100 μM. For the study of time-dependent aggregation, the peptide was dissolved in phosphate buffer at pH 7.5 to a final concentration of 10 μM. Subsequently, 30 μM vanadium complex was added to the peptide solution for comparison. 10 μM ThT was used as a fluorescence marker. The emission intensity at 484 nm was measured from 0 to 24 h

To identify the competitive binding of ThT and V complex to the peptide, firstly, the peptide was incubated for 24 h at 310 K, then the sample with different molar ratios of ThT was detected by the fluorescence to obtain a working curve and find a suitable concentration of ThT. Secondly, ThT in suitable concentration (40 μM for PrP106-126 and 60 μM for $A\beta_{1-42}$) was added to the incubated peptide to measure the initial fluorescence intensity. Thirdly, a series of vanadium complexes were added to the mixture and incubated together at 310 K for 24 h in phosphate buffer (pH=7.5). Then the mixture was determined by the fluorescence spectrometer as described above. The final concentration of the peptide was 10 μM, and the vanadium

complex used was 3, 6, 10, and 20 μM respectively. As for the detection of peptide aggregation influenced by the reductive agent, dithiothreitol (DTT) was added in the sample of aggregated peptide with vanadium complex in phosphate buffer at pH 7.5. After 24 h incubation of the mixture at 310 K, the sample was combined with ThT, and the emission intensity at 484 nm was measured. All data were obtained from the mean of three repeated experiments.

UV absorption spectra

UV spectra were acquired using a Cary 50 UV spectrometer (Varian, USA) at room temperature. A vanadium complex or independent ligand was dissolved in 5 mM phosphate buffer at pH 7.5 and the sample concentration was 50 μM. For the titration of vanadium complex to ThT, various concentrations of the compound (0, 2, 4, 6, 10, 15, 20, 50, and 100 μM) were added in 10 μM ThT solution. The scan wavelength was from 190 nm to 800 nm for each sample.

Circular dichroism analysis

Circular dichroism (CD) spectra were obtained using the samples prepared in 5 mM phosphate buffer at pH 7.5. After a 24 h incubation of the peptide at 310 K, different concentrations of the vanadium complexes were added. The mixing system underwent further incubation of 24 h at 310 K and it was detected by a Jasco J-810 spectropolarimeter (Japan Spectroscopy, Japan). The final concentration of peptide was 50 and 150 μM for the vanadium complexes. A 1 mm quartz cell was used for all CD measurements. The spectra were recorded between 190 and 250 nm with a 0.5 nm spectral step and 2 nm bandwidth. A scan rate of 100 nm min^{-1} with a 1 s response time was used. The baseline was subtracted by running the phosphate buffer alone or buffer containing the corresponding vanadium complex as blank. The ellipticity of the CD spectrum

was expressed in millidegrees (mdeg). Each spectrum represents an average of three accumulated scans.

Atomic force microscopy images

Samples were prepared by adding the metal complex to the peptide solution, which was then incubated at 310 K for 24 h. The final peptide concentration of each sample was 10 μM for PrP106-126 and 5 μM for $A\beta_{1-42}$. Atomic force microscopy (AFM) images were obtained in the tapping mode with a silicon tip under ambient condition, a scanning rate of 1 Hz, and a scanning line of 512. The AFM equipment used was a Veeco D3100 instrument (Veeco Instruments 151 Inc., USA).

Dynamic light scattering measurements

Dynamic light scattering (DLS) experiments were performed using a Zetasizer Nano instrument (Malvern Instruments, Worcestershire, UK). A 1 ml of 50 μM PrP106-126 solution with two peroxovanadium complexes (50 μM) was incubated at 310 K for 24 h and centrifuged at 12000 rpm for 10 min to remove large precipitates. The supernatants were transferred to a fluorescence cuvette for the measurements.

NMR measurements

^{1}H NMR spectra were obtained using a Bruker Avance 400 or 600 MHz spectrometer at 298 K. The samples were prepared by adding a stock solution of the metal compound to the peptide solution and data were acquired after 12 h of incubation. The final peptide concentration used was 0.25 mM. The metal compound used was 5.0 equivalent amounts of the peptide. The pH

value was carefully adjusted to 5.7 with either deuterium chloride (DCl) or sodium deuteroxide (NaOD). A Watergate pulse program with gradients was applied to suppress the residual water signal.

For the ^{1}H NMR experiment of PrP106-126 oxidation by hydrogen peroxide (H_2O_2), the final concentrations of peptide and H_2O_2 was 0.5 mM and 5mM, respectively. The mixing sample was measured by 600 MHz NMR spectrometer after 12h incubation. For the experiment of direct methionine oxidation by complex **1** and **2**, the concentration of methionine and metal complex was 0.5mM and 1.5 mM, respectively, and the detection was performed after 12 h incubation. To determine the reduction of oxidated peptide, a reductive agent DTT was added to the sample of peptide with vanadium complex. After a 12h incubation of the mixture, the ^{1}H NMR spectrum was acquired. All other conditions were same as mentioned above.

Electrospray ionization MS

The concentration of the peptide sample used in the electrospray ionization (ESI)-MS experiments was kept constant at 50 μM. Three or ten equivalent amounts of peroxovanadium complex were added to the sample of PrP106-126 or $A\beta_{1\text{-}42}$. The sample was incubated for 12 h before assay. ESI-MS spectra were recorded in the positive mode by directly introducing the samples at a flow rate of 3 μL min^{-1} in an APEX IV FT-ICR high-resolution MS (Bruker, USA) equipped with a conventional ESI source. The working conditions were as follows: end plate electrode voltage, −3500 V; capillary entrance voltage, −4000 V; skimmer, 1 and 30 V; and dry gas temperature, 473 K. The flow rates of the drying gas and the nebulizer gas were set at 12 and 6 L min^{-1}, respectively. Data analysis 4.0 software (Bruker) was used to acquire data. Deconvoluted masses were determined using an integrated deconvolution tool.

HPLC

The oxidation of PrP106-126 by vanadium complexes **1** and **2** was analyzed by reverse HPLC using an Agilent Technologies 1200 liquid chromatograph equipped with C18 column. The sample was loaded and eluted beginning with solvent A (0.1% trifluoroacetic acid [TFA]) and then solvent B (0.1% TFA/acetonitril). The gradient for each sample was 0%–10% in 2 min, 10%–50% in 20 min, and 50%–95% in 25 min.

MTT assay

Human SH-SY5Y neuroblastoma cells were cultured in a 1:1 mixture of Dulbecco's modified Eagle's medium and F12 medium supplemented with 10% fetal bovine serum, 2 mM glutamine, 100 U mL^{-1} penicillin, and 100 U mL^{-1} streptomycin. Cells were maintained at 310 K in a humidified incubator under 95% air and 5% CO_2. Cell survival was assessed by measuring the reduction of 3-(4,5-dimethylthiazol-2-yl)-2,5-diphenyltetrazolium bromide (MTT). A 50 μM PrP106-126 or 10 μM $A\beta_{1-42}$ was incubated for 24 h with or without a 10 μM peroxovanadium complex, and then the mixture was added to the cells. The cells were incubated with 10 μL of MTT at 310 K for 4 h after four days of reaction. The absorbance at 570 nm was recorded with a Cary 50 UV-vis spectrophotometer (Varian, Inc., USA). Each experiment was performed in quintuples. Data were calculated as percentages of untreated control values. Statistical analyses were performed by a one-way/Bonferroni ANOVA-post hoc test.[42,43]

Results

Synthesis of peroxovanadium complexes

Two peroxovanadium complexes, namely, ammonium (2,2′-bipyridine) oxodiperoxovanadate ($(NH_4)[VO(O_2)_2(bipy)]\cdot 4H_2O$) **(1)** and ammonium (1,10-phenanthroline) oxodiperoxovanadate ($(NH_4)[VO(O_2)_2(phen)]\cdot 2H_2O$) **(2)**, were synthesized and identified in this study according to the reported methods.[44] NMR spectra of the compounds are presented in Fig. S1 (ESI). The spectra of the products are in accordance with that in literature. Another vanadium complex, potassium oxalatooxodiperoxovanadate ($K_3[VO(O_2)_2(ox)]\cdot 2H_2O$) **(3)** (Scheme S1), was also prepared and identified for comparison.

Inhibition of peroxovanadium complexes on amyloid peptides aggregation

PrP106−126 is essential to PrP^{Sc} aggregation, which is correlated with the neurotoxicity of prion proteins. $A\beta_{1\text{-}42}$ may self-aggregate and form amyloid deposits as well, which is linked to AD. The aggregation of PrP106-126 and $A\beta_{1\text{-}42}$ can be monitored by the fluorescence dye ThT as a marker. As shown in Fig. 1A and 1B, the fluorescence spectrum exhibited strong signals when ThT bound to aggregated PrP106-126 and $A\beta_{1\text{-}42}$, respectively. However, the ThT emission intensity, which indicated the aggregation extent of amyloid peptides, was noticeably decreased after incubation of the vanadium complexes with the peptides. Thus, the aggregation of the two amyloid peptides was affected by vanadium complexes. The UV experiments were performed in consideration of possible energy transfer between peroxovanadium complexes and ThT. The peroxovanadium complex has no absorption at 484 nm (Fig. S2). When a different molar ratio of the vanadium compound was added in the ThT solution, no change in ThT absorption (484 nm) was found (Fig. S2). The results indicated that no energy transfer existed between the vanadium complexes and ThT. Hence, in the ThT assay, the decrease of emission intensity was related to the inhibitory effect of vanadium complex on amyloid peptide aggregation.

In addition, the influence of the vanadium complexes on two amyloid peptides aggregation was concentration dependent. The IC_{50} values of the compounds on peptide aggregation were obtained using the method reported earlier.[45,46] IC_{50} represents the concentration of vanadium complexes required to achieve 50% of their maximum effects on amyloid peptide aggregation. Table 1 shows the IC_{50} values of the two peroxovanadium complexes for PrP106-126 and $A\beta_{1-42}$, respectively. PrP106-126 aggregation was strongly inhibited by **1**, with an IC_{50} value of 2.9±0.2 μM. The peptide was also inhibited by **2**, with an IC_{50} value of 5.3±0.3 μM. Moreover, $A\beta_{1-42}$ aggregation was inhibited by **1** and **2**, with IC_{50} values of 22.0±2.4 and 15.1±1.6 μM, respectively.

To determine if peroxovanadium complexes can directly affect amyloidogenesis of PrP106-126 and $A\beta_{1-42}$, we monitored the time course of peptide aggregation in the absence and presence of the two peroxovanadium complexes by using ThT as a marker. This investigation may disclose the property of peptide aggregation and possible influence from exterior molecule. The experiment started using a freshly prepared sample mixed with ThT. The results showed the fibrillization of 50 μM PrP106-126 with a lag phase of 1 h. The fluorescence intensity at 0 h might be attributed to partially preformed aggregates of the peptide and ThT itself. However, this did not affect the observation of the aggregation process which was followed by a growing phase of 3.5 h to attain total equilibrium. When vanadium complex was added, the fibrillization was not detected even after 6 h. The phenomenon suggested that vanadium complex effectively delayed PrP106-126 aggregation (Fig. 1C). As for $A\beta_{1-42}$, the aggregation time scale was also changed by the vanadium complexes. The lag time was delayed from 1 h to approximately 7 h, and effective influence was observed (Fig. 1D). The ThT assay and time course results showed

that the two vanadium complexes affected the aggregation of PrP106-126 at a greater degree than that of $A\beta_{1-42}$.

However, the competition between ThT and vanadium complex might exist. In order to figure it out, a working curve of the fluorescence intensity representing peptide aggregation *via* ThT concentration was described (Fig. S3). Under the suitable ThT concentration, addition of vanadium complex induced a remarkable fluorescence decrease, which indicated a competition binding between ThT and vanadium complex to the amyloidogenic peptides.

Peptide conformational change induced by vanadium complexes

CD spectroscopy was employed to examine the effect of the vanadium complexes on the conformation of PrP106-126 and $A\beta_{1-42}$. The peptides (50 μM) with or without the vanadium complexes (150 μM) were incubated in 5 mM phosphate buffer at pH 7.5 for 24 h at 310 K. The CD spectrum of PrP106-126 showed a distinct negative signal at approximately 220 nm, which revealed that the β sheet conformation was the main component in the solution (Fig. 2A). The addition of vanadium complex remarkably influenced the secondary structure of PrP106-126 with a clear negative absorption shift at approximately 200 nm. The data indicated that the peptide conformation was changed notably by the interaction between the vanadium complexes and PrP106-126. Similarly, the CD spectrum of $A\beta_{1-42}$ also showed a negative absorption at approximately 220 nm, which suggested the formation of an aberrant β-sheet structure of $A\beta_{1-42}$ (Fig. 2B). The addition of vanadium complexes produced a negative signal at 198 nm, whereas the negative peak at 220 nm was obviously weakened. This phenomenon indicated a change in secondary structure of $A\beta_{1-42}$.

AFM and DLS analyses of peptide aggregation

AFM was employed to determine the effect of vanadium complexes on the morphology of peptide fibrillization. The self-assembly of PrP106-126 alone produced large aggregates after 24 h of incubation at 310 K, with a dense fibrillar structure (Fig. 3). In the presence of vanadium complexes, the peptide aggregation was inhibited significantly. The most remarkable morphological difference occurred with scarce granular/spherical oligomers while PrP106-126 was treated with the vanadium compounds. However, complexes 1 and 2 inhibited the aggregation of $A\beta_{1\text{-}42}$ to different extent when compared with PrP106-126. Although amyloid fibril formation was not observed, scattered granular/spherical oligomers were found.

The size distribution of PrP106-126 aggregates as supplement was determined by DLS after incubation of the peptide with and without the vanadium complexes. The hydrodynamic radius of PrP106-126 decreased and formed a polydisperse bimodal solution with average hydrodynamic diameters of 10 nm to 100 nm and 100 nm to 450 nm (Fig. 4A). These results were in accordance with the ThT fluorescence assay and AFM images. Accordingly, the results support the hypothesis that vanadium complexes strongly inhibit the formation of large aggregates and fibrils by PrP106-126. Furthermore, the vanadium complexes reduced the particle size of the aggregated $A\beta_{1\text{-}42}$ (Fig. 4B). Although some of the particles were 1–5 nm in size, the size of the majority of the particles was distributed around 500–1000 nm. As indicated by the AFM and DLS results, peroxovanadium complexes **1** and **2** have effects on PrP106-126 and $A\beta_{1\text{-}42}$ aggregation with different extents.

Specific interaction of peroxovanadium complexes with the peptides

PrP106-126 includes one histidine and two methionine residues, which are critical factors in metal binding and peptide aggregation.[47] ^{1}H NMR spectroscopy was used to monitor the proton resonance change of PrP106-126 in the absence and presence of two vanadium complexes to determine whether peroxovanadium complexes acted on these residues. The ^{1}H NMR spectrum of PrP106-126 was acquired, and the characteristic peaks from the side chains of His111 and Met 109/112 were identified as reported.[23,47] After incubation of the vanadium complex with PrP106-126, a slight decrease in the signal intensity at 7.38 ppm appeared, which was assigned to the $C_{\delta}H_{s}$ resonance of His111 (Fig. 5). Furthermore, the resonance peak from complex **1** was also observed to produce an intensity decrease, which should result from the change of proton relaxation property. The effect of complex **2** on peptide was similar to complex **1** (Fig. S4). The results implied a direct interaction of the peptide with the complex.

Aside from the mentioned above, a remarkable chemical shift from 2.08 ppm to 2.72 ppm was detected in the spectra, and the peak was assigned to the Met 109/112 side chain $C_{\varepsilon}H_{s}$ resonance. The chemical shift at 2.72 ppm matched the methyl resonance from dimethyl sulfoxide. The chemical shift indicated that the methionine residues may have been oxidized by the vanadium complex. The appearance of oxidation state (2.72 ppm) and reduction state (2.08 ppm) indicated a slow exchange NMR course.[48] As for $A\beta_{1\text{-}42}$, a new peak at 2.72 ppm appeared when 5.0 equivalent of metal compound was added in solution, which implied a homothetic methionine oxidation (Fig. 6). Moreover, the peak intensity from the complex decreased as well, which might be attributed to direct interaction of the compound with the peptide. (Fig. S5).

To verify the speculation of oxidation, we used the methionine molecule directly to interact with the vanadium complexes. Interestingly, the result was similar to what we found for PrP106-126 and $A\beta_{1\text{-}42}$; methionine oxidation occurred as detected by 1D ^{1}H NMR (Fig. S6).

Furthermore, by allowing H_2O_2 to interact with PrP106-126, a similar peak in 1D ^{1}H NMR spectrum appeared (Fig. S6). This finding suggested that peroxovanadium complexes may react with two amyloid peptides through methionine oxidation. In addition, the oxidation of vanadium complexes to the two peptides was time dependent, all above data were acquired after equilibration time.

ESI-MS was employed to analyze the mixture of PrP106-126 with vanadium complex and verify if the interaction between the peroxovanadium complexes and PrP106-126 could result in methionine oxidation. PrP106-126 showed two peaks, at 956.99(2+) and 638.33(3+), which correspond to the expected mass (Fig. S7). The addition of **1** caused the formation of adduct [PrP106-126+2O] [648.67 (3+)], which was accompanied with adducts [PrP106-126+$VO(O_2)_2$+$VO(O_2)_2$(bipy)] [778.60 (3+)] and [PrP106-126+$VO(O_2)_2$(bipy)] [1099.99(2+)]. Interestingly, the peak intensity of [PrP106-126+2O] was dominant, as shown in Fig. 7A. Combining the up-field change of the peak at 2.08 ppm in the NMR spectrum and the small molecule methionine oxidation by vanadium complexes (Fig. S6), the adduct of the double O atoms may arise from the oxidation of methionines 109 and 112 specifically. The addition of **2** produced the same adduct [PrP106-126+2O] as that of **1**, with another adduct [PrP106-126+$V(O_2)_2$(phen)] [736.33 (3+) and 1104.00 (2+)] (Fig. 7B). The adduct peak intensity in **2** was similar to findings in **1**, which implied the oxidation of methionine residues as a major interactive mode. The other adducts may be attributed to metal coordination or hydrophobic effects that accompanied the oxidation in the system, which was in agreement with that observed in NMR spectra.

MS spectra of $A\beta_{1-42}$ with **1** or **2** at a higher molar ratio were also obtained. $A\beta_{1-42}$ itself showed a MS peak at 4512.25(1+) as expected (Fig. S8). Addition of compound **1** and **2**

produced a new adduct peak at 4528.24(1+) and 4529.25(1+), respectively. $A\beta_{1-42}$ has only one methionine residue at position 35; the mass difference matched one oxygen atom adducted to the peptide. The two peroxovanadium complexes strongly inhibited the aggregation of PrP106-126 and $A\beta_{1-42}$ potentially by site-specific oxidation of methionines. Methionine oxidation was also reported to play a crucial role in amyloid peptide aggregation.[49,50] Peptide oxidation may be more critical than metal coordination and hydrophobic interaction between the vanadium compounds and amyloid peptides, as indicated by the NMR and MS results.

Plenty of studies have demonstrated that metal complexes with aromatic nitrogen-containing ligands are good candidates to treat amyloid protein aggregation. The peroxovanadium complexes **1** and **2** showed better inhibitory effects against peptide fibril formation. However, it is not clear if the effect mainly resulted from methionine oxidation. Herein, in order to identify the specific role of peroxovanadium complexes, another compound **3**, without aromatic ring and large ligand spatial effect, was selected to compare its inhibitory effect with **1** and **2**. PrP106-126 was incubated in the absence and presence of **3** at 310 K for 24 h and analyzed by ThT assay and AFM. The ThT fluorescence intensity decreased dramatically after adding the complex **3**. The AFM results showed the same effect as **1** and **2** without obvious fibrils and granular particles (Fig. S9). Aside from the investigation of the inhibitory action, our MS result proved the oxidation of PrP106-126 in the presence of **3**, owing to the formation of [PrP106-126+2O] adduct (data not shown). In addition, the inhibition of peptide aggregation induced by methionine oxidation was identified using H_2O_2. Incubation of H_2O_2 with the peptide resulted in the fluorescence intensity decrease at some extent as indicated by ThT assay (Fig. S10). Furthermore, the peptide oxidation induced by vanadium complex could not be effectively reversed using DTT, ass detected by NMR (Fig. S11). Meanwhile, ThT assay

revealed that DTT could not reverse the inhibitory effect of vanadium complexes on peptide aggregation (Fig. S12).

HPLC assay

To identify the interaction of amyloid peptide with vanadium complex, HPLC assay was employed in which PrP106-126 was used as an example. HPLC is an effective tool to observe the component change in amyloid proteins.[51] As shown in Fig. 8, the sample with PrP106-126 alone gave an elution time of ~14.6 min. With the addition of complex **1**, the elution time shortened to ~14.3 min and ~13.4 min. The peak at elution time ~10 min was detected from complex **1**, as observed in Fig. S13. Addition of complex **2** resulted in the shift of elution time to ~13.3 min and the peak observed at elution time of ~11 min was attributed to complex **2**. The earlier elution time revealed a component change which was induced by the interaction of the peptide with the vanadium complex. The results of NMR and ESI-MS indicated that the change may result from methionine oxidation and direct interactions.

Regulation of peroxovanadium complexes on neurotoxicity of PrP106−126 and $A\beta_{1-42}$

The peroxovanadium complexes could interact with PrP106-126 and $A\beta_{1-42}$, oxidize them, and regulate their aggregation behavior significantly. Furthermore, the ability of the complexes to reduce the neurotoxicity of PrP106-126 and $A\beta_{1-42}$ was assessed using human SH-SY5Y neuroblastoma cells. Cell survival was evaluated after treating the SH-SY5Y cells with the peptide alone or with the peptide and peroxovanadium complex. By using SH-SY5Y cells as a control (with 100% viability), PrP106-126 was found to decrease the cell viability remarkably to (57±0.2)%, as measured by the MTT assay (Fig. 9A). The addition of vanadium complex to

PrP106-126 rescued the cell viability to (80±0.5)% for **1** and (74±0.8)% for **2**. One-way ANOVA indicated that the detection was significant (at 95% level of significance) for PrP106-126 induced cytotoxicity. The detection was also significant for the rescued cell viability of vanadium complex. However, the difference in detection efficacy of the two vanadium complexes was nonsignificant.

Vanadium compounds are known to exhibit both toxic and beneficial effects on living systems. Although the cytotoxicity of peroxovanadium complexes to the SH-SY5Y cells could be detected (Fig. S14), they may restore the neurotoxicity induced by PrP106-126. Similarly, $A\beta_{1\text{-}42}$ caused a significant cell viability reduction of human SH-SY5Y neuroblastoma cells to (61±0.6)%. After incubation of the peroxovanadium complexes with $A\beta_{1\text{-}42}$, the cytotoxicity was decreased, with cell viability of (69±1.1)% for **1** and (73±1.9)% for **2** (Fig. 9B). The one-way ANOVA for $A\beta_{1\text{-}42}$ was analogous to that for PrP106-126. However, the difference of cell viability of these complexes to the two peptides seemed not so distinct from what they reflected by other experiments. The cells are a complicated system, and the present test could not deduce if vanadium complexes affected other components in the cells, and other interaction mechanism possibly existed.

Discussion

Different interactive efficacy of peroxovanadium complexes with PrP106-126 and $A\beta_{1\text{-}42}$

Peroxovanadium complexes regulated the aggregation of PrP106-126 and $A\beta_{1\text{-}42}$, as confirmed by the ThT assay and AFM. Both **1** and **2** inhibited amyloid fibril formation through interaction with the peptide. In addition, the peptide conformation was influenced notably as indicated by the CD spectra. Based on the distinct IC_{50} values, NMR data, and DLS analysis, the effects of the

two compounds on PrP106-126 aggregation were more remarkable than their effects on $A\beta_{1-42}$. This may be attributed to the different molecular structures of the complex, methionine oxidation, hydrophobic interaction, and possible metal coordination. Moreover, complex **3**, which has no aromatic ligand, was used in this study to identify if peroxovanadium stimulates the oxidation of methionine in the peptide or if the inhibitory effect from the ligand is predominant. The results obtained from the use of complex **3** verified the role of peroxovanadium. Methionine oxidation may be an important factor in the inhibition of amyloid peptides aggregation, besides the direct interaction of the compound with the peptide. NMR data showed the remarkable change in the methionine side chain, which was assigned to the oxidation of methionine to methionine sulfoxide. The speculation was confirmed by the MS data and independent methionine oxidation experiments, which elucidated a crucial action mode of the vanadium complexes with amyloid peptides through methionine oxidation.

Site-specific methionine oxidation

Although a previous study has demonstrated that peroxovanadium complexes affect hIAPP fibrillization mainly through hydrophobic and electrostatic interactions,[41] the present work suggested that methionine oxidation may play a significant role in the peptide aggregation. Vanadium complexes had better interaction but different efficacy to the two amyloid peptides, because of their different sequences. $A\beta_{1-42}$ contains one methionine residue at position 35 that can be oxidized by hydrogen peroxide.[52,53] The action mode of peroxovanadium complex differs from those of metal complex inhibitors reported for PrP106-126, in which metal coordination occupies a predominant position.[23,54,55] Methionine oxidation appears to be a significant factor in fibril formation of amyloid proteins and affects the pathogenic aggregation of some amyloid

proteins, such as α-synuclein, Aβ and PrP.[56–58] Several studies have indicated that the oxidation of methionine drastically affects protein structure because of the higher polarity and lower flexibility of methionine sulfoxide than that of the methionine side chain.[59–62] As a result, peptide aggregation is significantly affected. Interestingly, the present study demonstrated the methionine oxidation of two peptides by peroxovanadium complexes, and the inhibitory effect of the compounds against peptide aggregation was prominent, combining the MS and NMR data with ThT assay and AFM images. The results may also be verified by complex **3** and H_2O_2, from their effects on peptide aggregation. Furthermore, the neurotoxicity induced by the two peptides was better rescued by the vanadium complexes. The results were not completely in accordance with that observed on the inhibition of peptide aggregation, because the mechanism of cytotoxicity was complicated and it could not be elucidate at present.

Conclusion

In summary, this study investigated the interaction of peroxovanadium complexes with amyloid peptides PrP106-126 and $A\beta_{1\text{-}42}$. Our results indicated that the selected peroxovanadium complexes inhibited the formation of amyloid fibril, postponed their aggregation process, and changed the conformation of the peptides. NMR, MS, and ThT assay results indicated enhanced interactive efficacy of the vanadium complexes and the two peptides. The two peroxovanadium complexes have inhibitory effects on PrP106-126 and $A\beta_{1\text{-}42}$ aggregation with different extents. The interactions also provided neuroblastoma cells with a high viability to both peptides. Particularly, this work provided credible evidence that peroxovanadium complexes induced the site-specific oxidation of methionine residues, besides direct interaction between the complex and the peptide. The interaction mechanism of peroxovanadium complexes with PrP106-126 and

$A\beta_{1-42}$ are somewhat different from those of existing metal complex inhibitors, such as platinum and ruthenium complexes which mainly depend on the function of metal coordination. Our results provide evidence of the potential of metal complexes for treatment of amyloid fibrillization. The findings of this study can be applied in designing relevant therapeutics against amyloid diseases.

Acknowledgements

The work was supported by the National Natural Science Foundation of China (No. 21271185 and No. 21473251), and the National Basic Research Program (No. 2011CB808503).

References

1 D. J. Selkoe, *Physiol. Rev.,* 2001, **81,** 741-766.

2 K. Conway, S. J. Lee, J. C. Rochet, T. Ding, J. Harper, R. Williamson, P. Lansbury, *Ann. NY Acad. Sci.,* 2000, **920,** 42-45.

3 G. Cooper, A. Willis, A. Clark, R. Turner, R. Sim, K. Reid, *Proc. Natl. Acad. Sci. U.S.A.,* 1987, **84,** 8628-8632.

4 F. Chiti, C. M. Dobson, *Annu. Rev. Biochem.,* 2006, **75,** 333-366.

5 S. B. Prusiner, *Science,* 1997, **278,** 245-251.

6 G. Forloni, N. Angeretti, R. Chiesa, E. Monzani, M. Salmona, O. Bugiani, F. Tagliavini, *Nature,* 1993, **362,** 543-546.

7 S. B. Prusiner, *Proc. Natl. Acad. Sci. U.S.A.,* 1998, **95**, 13363-13383.

8 P. Walsh, K. Simonetti, S. Sharpe, *Structure,* 2009, **17,** 417-426.

9 M. Salmona, P. Malesani, L. De Gioia, S. Gorla, M. Bruschi, A. Molinari, F. Della Vedova, B. Pedrotti, M. Marrari, T. Awan, *Biochem. J.,* 1999, **342**, 207-214.

10 S. Vilches, C. Vergara, O. Nicolás, G. Sanclimens, S. Merino, S. Varón, G. A. Acosta, F.

Albericio, M. Royo, J. A. Del Río, *PloS ONE,* 2013, **8,** e70881.

11 C. N. O'Donovan, D. Tobin, T. G. Cotter, *J. Biol. Chem.,* 2001, **276,** 43516-43523.

12 T. Florio, M. Grimaldi, A. Scorziello, M. Salmona, O. Bugiani, F. Tagliavini, G. Forloni, G. Schettini, *Biochem. Bioph. Res. Commun.,* 1996, **228,** 397-405.

13 T. Florio, S. Thellung, C. Amico, M. Robello, M. Salmona, O. Bugiani, F. Tagliavini, G. Forloni, G. *J.* Schettini, *Neurosci. Res.,* 1998, **54,** 341-352.

14 L. Vella, A. F. Hill, R. Cappai, Mechanisms of Prion Toxicity and Their Relationship to Prion Infectivity, in *Neurodegeneration and Prion Disease*, Springer, 2005, pp 217-240.

15 R. Gellman, J. Gibson, *Nature,* 1996, **380,** 28.

16 D. Brown, *Biochem. J.,* 2000, **352,** 511-518.

17 N. Singh, Y. Gu, S. Bose, S. Kalepu, R. Mishra, S. Verghese, *Frontiers in bioscience: a journal and virtual library,* 2002, **7,** a60-71.

18 C. Selvaggini, L. Degioia, L. Cantu, E. Ghibaudi, L. Diomede, F. Passerini, G. Forloni, O. Bugiani, F. Tagliavini, M. Salmona, *Biochem. Bioph. Res. Commun.,* 1993, **194,** 1380-1386.

19 Y. Porat, A. Abramowitz, E. Gazit, *Chem. Biol. Drug Des.,* 2006, **67,** 27-37.

20 M. Tatarek-Nossol, L. M. Yan, A. Schmauder, K. Tenidis, G. Westermark, A. Kapurniotu, *Chem. Biol.,* 2005, **12,** 797-809.

21 K. J. Barnham, V. B. Kenche, G. D. Ciccotosto, D. P. Smith, D. J. Tew, X. Liu, K. Perez, G. A. Cranston, T. J. Johanssen, I. Volitakis, *Proc. Natl. Acad. Sci. U.S.A.,* 2008, **105,** 6813-6818.

22 L. He, X. Wang, C. Zhao, H. Wang, W. Du, *Metallomics,* 2013, **5,** 1599-1603.

23 X. Wang, L. He, C. Zhao, W. Du, J. Lin, *J. Biolog. Inorg. Chem.,* 2013, **18,** 767-778.

24 K. J. Barnham, A. I. Bush, *Chem. Soc. Rev.,* 2014, **43**, 6727-6749.

25 W. J. Geldenhuys, C. J. Van der Schyf, *Curr. Mde. Chem.,* 2013, **20**, 1662-1672.

26 D. J. Hayne, S. Li, P. S. Donnelly, *Chem. Soc. Rev.,* 2014, **43**, 6701-6715.

27 G. Grasso, S. Bonnet, *Metallomics,* 2014, **6**,1346-1357.

28 E. L. Tolman, E. Barris, M. Burns, A. Pansini, R. Partridge, *Life Sci.,* 1979, **25,** 1159-1164.

29 G. R. Willsky, K. Halvorsen, M. E. Godzala, L.-H. Chi, M. J. Most, P. Kaszynski, D. C. Crans, A. B. Goldfine, P. J. Kostyniak, *Metallomics*, 2013, **5,** 1491-1502.

30 D. Rehder, *Fut. Med. Chem.,* 2012, **4,** 1823-1837.

31 D. Rehder, *Inorg. Chem. Commun.,* 2003, **6,** 604-617.

32 M. Li, W. Ding, J. J. Smee, B. Baruah, G. R. Willsky, D. C. Crans, *Biometals,* 2009, **22,** 895-

905.

33 H. Sakurai, *Chem. Rec.,* 2002, **2,** 237-248.

34 J. Gätjens, B. Meier, T. Kiss, E. M. Nagy, P. Buglyo, H. Sakurai, K. Kawabe, D. Rehder, *Chem.-Eur. J.,* 2003, **9,** 4924-4935.

35 B. I. Posner, R. Faure, J. W. Burgess, A. P. Bevan, D. Lachance, G. Zhang-Sun, I. G. Fantus, J. B. Ng, D. A. Hall, B. S. Lum, *J. Biol. Chem.,* 1994, **269,** 4596-4604.

36 J. H. Hwang, R. K. Larson, M. M. Abu-Omar, *Inorg. Chem.,* 2003, **42,** 7967-7977.

37 J. Benítez, L. Guggeri, I. Tomaz, G. Arrambide, M. Navarro, J. C. Pessoa, B. Garat, D. Gambino, *J. Inorg. Biochem.,* 2009, **103,** 609-616.

38 J. Benítez, L. Becco, I. Correia, S. M. Leal, H. Guiset, J. C. Pessoa, J. Lorenzo, S. Tanco, P. Escobar, V. Moreno, *J. Inorg. Biochem.,*2011, **105,** 303-312.

39 T. L. Turner, V. H. Nguyen, C. C. McLauchlan, Z. Dymon, B. M. Dorsey, J. D. Hooker, M. A.

Jones, *J. Inorg. Biochem.,* 2012, **108,** 96-104.

40 O. J. D'Cruz, Y. Dong, F. M. Uckun, *Biochem. Bioph. Res. Commun.,* 2003, **302,** 253-264.

41 L. He, X. Wang, C. Zhao, D. Zhu, W. Du, *Metallomics,* 2014, **6,** 1087-1096.

42 T. N. Martinez, X. Chen, S. Bandyopadhyay, A. Merrill, M. G. Tansey, *Mol. Neurodegener.,* 2012, **7,** 45-53.

43 R.S. Akhtar, Y. Geng, B. J. Klocke1, K. A. Roth, *Cell Death Differ.,* 2006, **13,** 1727–1739.

44 N. Vuletić, C. J. Djordjević, *Chem. Soc., Dalton Trans.,* 1973, **11,** 1137-1141.

45 J.H. Byun, H.Y. Kima, Y.S. Kima, I.M. Jung, D.J. Kim, W.K. Lee, K.H. Yoo, *Bioorg. Med. Chem. Lett.,* 2008, **18,** 5591–5593.

46 V.P.S. Chauhan, I. Ray, A. Chauhan, J. Wegiel, H.M. Wisniewski, *Neurol. Res.,* 1997, **7,** 805–809.

47 E. Gaggelli, F. Bernardi, E. Molteni, R. Pogni, D. Valensin, G. Valensin, M. Remelli, M. Luczkowski, H. Kozlowski, *J. Am. Chem. Soc.,* 2005, **127,** 996-1006.

48 M.P. Williamson, *Prog. Nucl. Mag. Res. Sp.,* 2013, **73,** 1-16.

49 K.J. Binger, M.D.W. Griffin, G.J. Howlett, *Biochemistry* , 2008, **47,** 10208-10217.

50 S. Nishino, Y. Nishida, *Inorg. Chem. Commun.,* 2001, **4,** 86-89.

51 J.R. Requenaa, M.N. Dimitrovaa, G. Legnameb, S. Teijeirae, S.B. Prusiner, R.L. Levinea, *Arch. Biochem. Biophys.,* 2004, **432,** 188-195.

52 L. M. Hou, I. Kang, R. E. Marchant, M.G. Zagorski, *J. Biol. Chem.,* 2002, **277,** 40173-40176.

53 L. M. Hou, H. Y. Shao, Y. B. Zhang, H. Li, N. K. Menon, E. B. Neuhaus, J. M. Brewer, I. J. L. Byeon, D. G. Ray, M. P. Vitek, T. Iwashita, R. A. Makula, A. B. Przybyla, M. G. Zagorski, *J. Am. Chem. Soc.,* 2004, **126,** 1992-2005.

54 Y. L. Wang, J. Xu, L. Wang, B. B. Zhang, W. H. Du, Chem.-Eur. J., 2010, 16, 13339-13342.

55 G. Ma, F. Huang, X. Pu, L. Jia, T. Jiang, L. Li, Y. Liu, Chem. -Eur. J., 2011, 17, 11657-11666.

56 M. Grabenauer, C. Wu, P. Soto, J. E. Shea, M. T. Bowers, J. Am. Chem. Soc., 2010, 132, 532-539.

57 V. N. Uversky, G. Yamin, P. O. Souillac, J. Goers, C. B. Glaser, A. L. Fink, FEBS Lett., 2002, 517, 239-244.

58 W. Vogt, Free Radic. Biol. Med., 1995, 18, 93-105.

59 L. Breydo, O. V. Bocharova, N. Makarava, V. V. Salnikov, M. Anderson, I. V. Baskakov, *Biochemistry,* 2005, **44,** 15534-15543.

60 M. J. Davies, *BBA-Proteins Proteom.,* 2005, **1703,** 93-109.

61 M. C. Miotto, E. E. Rodriguez, A. A. Valiente-Gabioud, V. Torres-Monserrat, A. S. Binolfi, L. Quintanar, M. Zweckstetter, C. Griesinger, C.O. Fernández, *Inorg. Chem.,* 2014, **53,** 4350-4358.

62 S. D. Maleknia, N. Reixach, J. N. Buxbaum, *FEBS J.,* 2006, **273,** 5400-5406.

TABLE

Table 1. IC_{50} values for the inhibition of vanadium complexes on aggregation of PrP106-126 and $A\beta_{1-42}$.

Vanadium complexes	**IC_{50} values (μM) [a]**	
	PrP106-126	$A\beta_{1-42}$
$(NH_4)[VO(O_2)_2(bipy)]\cdot 4H_2O$, 1	2.9±0.2	22.0±2.4
$(NH_4)[VO(O_2)_2(phen)]\cdot 2H_2O$, 2	5.3±0.3	15.1±1.6

[a] Data measured by the ThT fluorescence.

Figure captions

Scheme 1. The molecular structure of peroxovanadium complexes $(NH_4)[VO(O_2)_2$-(bipy)]·$4H_2O$ **1**, and $(NH_4)[VO(O_2)_2(phen)]·2H_2O_2$ **2**.

Fig. 1. Evaluation of the ability of V complexes to inhibit amyloid protein aggregation as measured by ThT fluorescence at 10 mM phosphate buffer pH=7.5. (A) PrP106-126 was incubated in the absence (black) and presence of **1** (red) and **2** (blue). (B) $A\beta_{1-42}$ was incubated in the absence (black) and presence of **1** (red) and **2** (blue). After incubation at 310 K for 24 h, ThT was added to each sample, and the determination was performed at room temperature. The sample of ThT alone is shown in gray. Then, the time scale experiments for PrP106-126 (C) and $A\beta_{1-42}$ (D). ThT fluorescence was monitored at 484 nm during peptide aggregation in the absence (black) and presence of **1**(red) and **2** (blue) at 10 mM phosphate buffer pH = 7.5. The concentrations of peptide and ThT were 10 μM both. The concentrations of vanadium complexes **1** and **2** were 30 μM both.

Fig. 2. CD spectra of peptide PrP106-126(A) and $A\beta_{1-42}$ (B) in the absence (black) and presence of **1** (red) and **2** (blue) at 5 mM phosphate buffer pH =7.5. The incubation was run for 24 h at 310 K, and the determination was performed at room temperature. The final concentration of peptide was 50 and 150 μM for the vanadium complexes.

Fig. 3. AFM morphology of PrP106-126 and $A\beta_{1-42}$ fibrils in the absence (A_1 and B_1) and presence of **1**(A_2 and B_2) and **2** (A_3 and B_3) at 5 mM phosphate buffer pH = 7.5. The final peptide concentration of each sample was 10 μM for PrP106-126 and 5 μM for $A\beta_{1-42}$. The concentration of vanadium complex was same as the peptide used. The scale bar is 500 nm.

Fig. 4. DLS analysis of the multimodal size distribution of amyloid aggregates in the absence (black) and presence of **1** (red) and **2** (blue). (A) PrP106-126; (B) Aβ1-42. The solution of 50 μM peptide with two peroxovanadium complexes (50 μM) was incubated at 310 K for 24 h before further detection.

Fig. 5. ^{1}H NMR spectra of PrP106-126 in 9:1 H_2O/D_2O at pH 5.7, 298 K. (A) PrP106–126 alone; (B) 0.25mM PrP106-126 in the presence of **1** (5.0 equiv); (C) complex **1** itself. The signal at 2.08 ppm (star) representing the $C_\delta H_s$ group of methionine is significantly shifted when incubated with the complex. The resonance peak at 7.38 ppm (dot) represents the $C_\delta H_s$ of His111, which is clearly perturbed by addition of V complex. The resonance peak at 8.70 ppm from the compound (inverted triangle) was also perturbed, which implied the interaction of vanadium complex with the peptide.

Fig. 6. The up-field portion of ^{1}H NMR spectra for $A\beta_{1\text{-}42}$ in the absence (A) and presence of V complex **1** (B) and **2**(C)**.** The peak at 2.05 ppm (inverted triangle) is from the methyl resonance of unoxidized methionine, while the peak at 2.72 ppm (dot) is assigned to the methyl resonance of oxidized methionine. The concentration of $A\beta_{1\text{-}42}$ in solution was 0.2 mM, and the vanadium complex used was 1.0 mM. The data was acquired after 12h incubation.

Fig. 7. ESI-MS spectra of PrP106−126 in the presence of **1** (A) and **2** (B). The peptide was kept constant at 50 μM. Three equivalent amounts of peroxovanadium complex were added to the sample of PrP106-126. The determination was performed after 12h incubation.

Fig. 8. HPLC trace of PrP106-126 in the absence (A) and presence of vanadium complex **1**(B) and **2**(C). The concentration of PrP106-126 used was 50 μM, and the vanadium complex used was 100 μM. The determination was performed after 24h incubation.

Fig. 9. (A) Cell viability monitored by the MTT assay. SH-SY5Y cells were treated with (grey) or without PrP106-126 (50 μM) (black), or treated with PrP106-126 and different peroxovanadium complexes (10 μM). The data are shown as means ± S.E.M. with n=5. $^{*}p<0.05$ (by one-way/ Bonferroni ANOVA-post hoc test). (B) Cell viability monitored by the MTT assay. SH-SY5Y cells were treated with (grey) or without $A\beta_{1\text{-}42}$ (10 μM) (black), or treated with $A\beta_{1\text{-}42}$ and different peroxovanadium complexes (10μM). The data are shown as means ± S.E.M. with n=5. $^{*}p<0.05$ (by one-way/ Bonferroni ANOVA-post hoc test).